

# Brown/Beige Fat Activation after Skeletal Muscle Ischemia-Reperfusion Injury

M. Liu<sup>1,2</sup>, Z. Wang<sup>1,3</sup>, C. S. Lee<sup>1,2</sup>, C. Nguyen<sup>1,2</sup>, L. Lee<sup>1</sup>, H. T. Kim<sup>1,2</sup>, B. T. Feeley<sup>1,2</sup>, X. Liu<sup>1,2</sup>

<sup>1</sup> Department of Veterans Affairs, San Francisco Veterans Affairs Medical Center, USA

<sup>2</sup> Department of Orthopaedic Surgery, University of California at San Francisco, California, USA

<sup>3</sup> Department of Orthopaedic Surgery, Third Xiangya Hospital of Central South University, Changsha, Hunan Province, China

## CORRESPONDING AUTHOR:

Xuhui Liu  
San Francisco Veterans Affairs  
Medical Center  
1700 Owens Street  
San Francisco, CA 94138  
E-mail: Liu.xuhui@ucsf.edu

## DOI:

10.32098/mltj.04.2020.05

## LEVEL OF EVIDENCE: 2B

## LIST OF ABBREVIATIONS

IRI: Ischemia-Reperfusion Injury  
BAT: Brown/Beige Adipose Tissue  
KO: Knockout  
UCP-1: Uncoupling Protein -1  
WAT: White Adipose Tissue  
WT: Wild Type  
TA: Tibialis Anterior  
PFA: Paraformaldehyde

## SUMMARY

**Objective.** Skeletal muscle Ischemia-Reperfusion Injury (IRI) is a commonly seen orthopedic injury. However, the role of The Brown/Beige Adipose Tissue (BAT) in muscle regeneration after IRI remains unknown. In this study, we assessed the role of BAT in muscle regeneration using UCP-1 reporter and Knockout (KO) mice. We hypothesize that UCP-1 expression increases in BAT after muscle injury and UCP-1 KO mice have reduced muscle regeneration after IRI.

**Methods.** Unilateral hindlimb IRI was performed on mice by applying a rubber band on the thigh for three hours. Amibegron and antagonist, which activates/deactivates BAT, were also given to mice after IRI. DigiGait analysis was performed at 2 or 4 weeks after IR injury. White (epididymal) fat, brown (interscapular) fat, beige (inguinal) fat and gastrocnemius muscles on both injury and contralateral uninjured sides were harvested. Muscle regeneration index, RT-PCR were performed on brown, beige and white fat to evaluate promyogenic growth factor gene expression.

**Results.** After hindlimb IRI, UCP-1 expression increased in brown, beige and white fat, which was accompanied by increase of gene expression promyogenic growth factors of IGF1 and follistatin. IRI also induced UCP-1 expression in both injured and contralateral uninjured muscle. DigiGait analysis demonstrated significantly decreased ( $p < 0.05$ ) hindlimb function at 2 weeks post-injury in UCP-1 KO mice compared to wildtype mice. Muscle histology showed significantly reduced muscle regeneration in UCP-1 KO mice compared to WT mice. Amibegron activates BAT and improves muscle regeneration, while SR-59230A deactivates BAT and reduced muscle regeneration after IRI.

**Conclusions.** BAT plays an important role in muscle regeneration of IRI. Pro-myogenic batokines from BAT may be the mediator for muscle regeneration after IRI.  $\beta_3$  adrenergic receptor agonists may be novel treatment for muscle IRI in the future.

## KEY WORDS

*Brown fat; beige fat; ischemia-reperfusion injury; muscle; regeneration; uncoupling protein-1.*

## INTRODUCTION

Skeletal muscle Ischemia-Reperfusion Injury (IRI) is a common and frequently serious complication of limb crush injuries, compartment syndrome, and vascular injuries (1). Deficient blood flow causes muscle lesions of structure disorganization and myocytes degeneration. Although prompt reperfusion restores the delivery of oxygen and substrates required for aerobic ATP generation and normalizes extracellular pH, reperfusion itself appears to have detrimental

consequences. Reperfusion accelerates the development of necrosis of muscle. Reactive Oxygen Species (ROS), cytokines, and chemokines from re-perfused muscle, as well as macrophages and mast cells, neutrophils migrated to muscle are thought to be the underlying mechanism of muscle IRI (2).

Humans and many other mammals have two distinct types of fat: white and brown fat. Recent studies revealed a third interchangeable form of fat named beige fat. Though

morphologically similar to white fat, beige fat can differentiate into brown fat by expressing the hallmark molecular signature of brown fat, Uncoupling Protein 1 (UCP-1), under certain conditions (3). Beyond their metabolic role, Beige/Brown Adipose Tissue (BAT) has been identified as an endocrine organ, which secretes various growth factors, known as batokines, including myogenic trophic factors, that have a role in promoting muscle growth and SC population expansion (4). Both adipose tissue and skeletal muscle are the largest organs in the body. Fat-muscle interaction has been gaining increasing attention recently. Adipose tissue and skeletal muscle secrete a large range of bioactive proteins, namely adipokines and myokines. Adipokines and myokines are involved in autocrine/paracrine interactions within adipose tissue and muscle, as well as in an endocrine cross-talk to other tissues (5).

$\beta$ 3 adrenergic receptors are mainly found in brown adipose tissue, beige adipose tissue, white adipose tissue, myocardium, skeletal muscle and liver (6).  $\beta$ 3 adrenoceptor agonists, Amibegron (SR 58611A) have been used as antidepressants in clinical trials. Amibegron can have effects on BAT mitochondrial multiplication along with energy expenditure. More interestingly, Amibegron can cause the fast changes occurring in Uncoupling Protein 1 (UCP-1) intrinsic action that is secondary to sympathetic stimulation and restore the brown adipocytes (7).

However, the role of BAT in muscle regeneration after IRI remains unknown. In this study, we assessed the role of brown, beige and white adipose tissue in muscle regeneration after IRI using UCP-1 reporter and Knockout (KO) mice. Moreover, Amibegron was also given to the mice to assess the role of UCP-1 in skeletal muscle recovery. We hypothesize that beige fat undergoes the “browning” process after IRI, and UCP-1 KO mice have impaired muscle regeneration after IRI compared to wildtype mice due to a lack of functional BAT.

## MATERIAL AND METHODS

### Unilateral hindlimb ischemia-reperfusion injury (IRI)

Unilateral hindlimb IRI was performed on 15 four months old male UCP-1<sup>luc2-tdTomato</sup> reporter mice (Jackson Laboratory Inc. Cat# 026690) using a calibrated 1/8 inch orthodontic latex elastic rubber band (6 ounces, Masel Orthodontics, Inc., Carlsbad, CA) as described previously (8). In brief, after general anesthesia by 1-5% isoflurane, a rubber band was applied and removed 3 hours later to allow reperfusion to the hindlimb. Mice were sacrificed at time points of 1, 2 and 4 weeks after injury. The number of animals required

for this study was determined based upon power analysis using our approximation of true effect and anticipated sample variability using the assumption:  $\alpha=0.05$ ,  $\beta=0.80$  with the outcome of a 20% difference in gait and histology. With these calculations, we determined that 5 mice per group would be sufficient to demonstrate significant differences between the control and treatment groups (n=5 per time point per group). Five un-injured UCP-1 reporter mice were used as the controls. The same IRI procedure was also applied to UCP-1 WT (n=5) and UCP-1 KO (Jackson Laboratory Inc. Cat# 003124) mice (n=5). Mice were harvested at 2 weeks after IRI after gait analysis. For Amibegron test,  $\beta$ 3 adrenergic receptor agonist (Amibegron), which activates BAT, was given at 10 mg/kg I.P. daily to wildtype mice (n=5) after IRI for 4 weeks. All animal care protocols were in compliance with our Institutional Animal Care and Use Committee (IACUC) (IACUC approved protocol# KIM17-017). Our study meets the ethical standards of the journal of MLTJ (9).

### Gait Analysis

DigiGait™ (Mouse Specifics Inc., Quincy, Massachusetts) analysis was performed to measure hindlimb function at 2 weeks and 4 weeks after IRI as described previously (10). All mice walked at 10 cm/s for 10 s on the DigiGait system. Swing Stride, Stance Stride, Brake Stride and Stance/Swing ratio were recorded to assess hindlimb function.

### Muscular and adipose tissue harvesting and wet muscle weight

After animals were sacrificed, white (epididymal) fat, brown (interscapular) fat, beige (inguinal) fat and Tibialis Anterior (TA) muscles on both injury and contralateral side were harvested. Wet weight of TA muscles was measured immediately after harvesting. Fat samples were fixed with 4% Paraformaldehyde (PFA), dehydrated with 30% sucrose and embedded in Paraffin (Leica Biosystems, IL). Muscle samples were flash-frozen in liquid nitrogen cooled isopentane. Both fat and muscles were cyrosectioned with a cryotome.

### Histology

TA muscles from the injury and contralateral sides were sectioned at 7  $\mu$ m with Microm HM550 cyrosection (Thermo Fisher,) at the muscle belly. Sections were fixed with 4% PFA (Sigma, St. Louis, MO) for 20 minutes at room temperature and blocked with 5% BSA (Jackson Immuno Research Laboratories) in PBS. Sections were permeated

with 100% methanol (Lot # B0533756, ACROS Organic) at -20 °C for 6 min, rinsed with PBS and incubated with primary antibody laminin (L9393, Lot# 028M-4890V, Sigma, MO, USA) diluted 1:500 in 5% BSA at 4 °C overnight. After rinsing in PBS three times, sections were incubated at room temperature for 1 h with secondary antibody (donkey anti-rabbit conjugated to Alexa Fluor®-647 1/500, ab150075, Lot# GR3191436-2, Abcam) diluted in 5% BSA. After rinsing in PBS three times, coverslip was laid on and slides were sealed with Vectashield (H-1000, Vector Laboratories). Slides were then observed on an optical microscope (Zeiss, Oberkochen, Germany). Pictures were taken and analyzed using Bioquant (Nashville, TN, USA). All pictures were assessed by two blinded researchers. Muscle regeneration was evaluated by regeneration index (% of regenerating fibers with central nuclei among total fibers). Cross sections area was measured by for muscle fibers in five randomly selected areas on sections from mid-bellies of TA muscle. 600 to 2000 fibers in each sample were calculated using Bioquant (Nashville, TN, USA).

PFA fixed adipose tissue sections were processed with Benchtop Tissue Processor (Leica TP1020) and embedded in paraffin according to routine histologic techniques (Medites TES 99). Sections, 5- $\mu$ m thick, were stained with DAPI and sealed with 10% glycerin till they were being ready to image.

### Luciferase assay

UCP-1 gene expression level was also measured by Luc2 reporter gene with luciferase in fat tissue from UCP-1 reporter mice. Briefly, adipose tissue was fast frozen in liquid nitrogen and homogenized with 0.5 ml/100 mg lysis buffer using tissue grinder. The mixture was frozen and thawed in the -80 °C and 37 °C for 3 cycles. The solution was centrifuged at 4000 RPM for 5 minutes. Finally, the supernatant was collected and stored in -80° C until ready to analyze. Luciferase in fat lysate was measured with Luciferase assay System (E1501, Promega, Italy) as described previously (11). 100  $\mu$ l of fat lysate supernatant were placed in 96 well plate and 200  $\mu$ l of substrate and buffer were added

into each well. Each sample was measured in triplicate. The plates were read by Bio-rad plate reader with luminometer for 10 seconds.

### Reverse-Transcript Polymerase Chain Reaction (RT-PCR)

Total RNA for both brown (n=5 per group), beige (n=5 per group) and white (n=5 per group) was extracted using Trizol reagent (Fisher Scientific, CA, USA) according to the manufacture's instruction. Transcription First Strand cDNA Synthesis Kit (Roche Applied Bioscience Inc., Indianapolis, IN, USA) was applied to synthesize cDNA. RT-PCR was performed to quantify gene expression of using SYBR Green Detection and an Applied Biosystems Prism 7900HT detection system (Applied Biosystems, Inc., Foster City, CA). Brown fat markers UCP-1 and PRDM-16, promyogenic batokines of follistatin and IGF1 gene expression were analyzed via RT-PCR. Sequences of the primers for target genes were showed in **table I**. The expression level of each gene was normalized to that of the house-keeping gene of R26. Folds changes relative to naive control group were calculated by  $\Delta\Delta$ CT.

### Statistical analysis

A Student t-Test was performed to determine a significant difference between UCP-1 KO and wildtype mice (cross section area, regenerated fiber index) as well as between Amibegron and Dimethyl Sulfoxide (DMSO) treated group (cross section area, regenerated fiber index). Statistical significance was considered when  $p < 0.05$ .

## RESULTS

### UCP-1 were activated in adipose tissue and muscle after IRI

UCP-1 signal was detected in all adipose tissue after IRI. The UCP-1 signal of brown, beige and white adipose tissue

**Table I.** Primers used for qRT-PCR.

Gene	Forward (5'→3')	Reverse (5'→3')
Rps26	ACGGGAAACCCATCACCATC	CCCTTCCACGATGCCAAAGT
Fst-288	CTCTCTCTGCGATGAGCTGTGT	GGCTCAGGTTTTACAGGCAGAT
Fst-315	CTCTCTCTGCGATGAGCTGTGT	TCTTCCTCCTCCTCCTCTCCT
IGF-1	AAAGCAGCCCCGCTCTATCC	CTTCTGAGTCTTGGGCATGTCA
UCP1	ACTGCCACACCTCCAGTCATT	CTTGCCTCACTCAGGATTGG
PRDM16	CCCAGTTTAACCTGTTTGTAGGCA	ATCCGCCATTGTTAAGACC

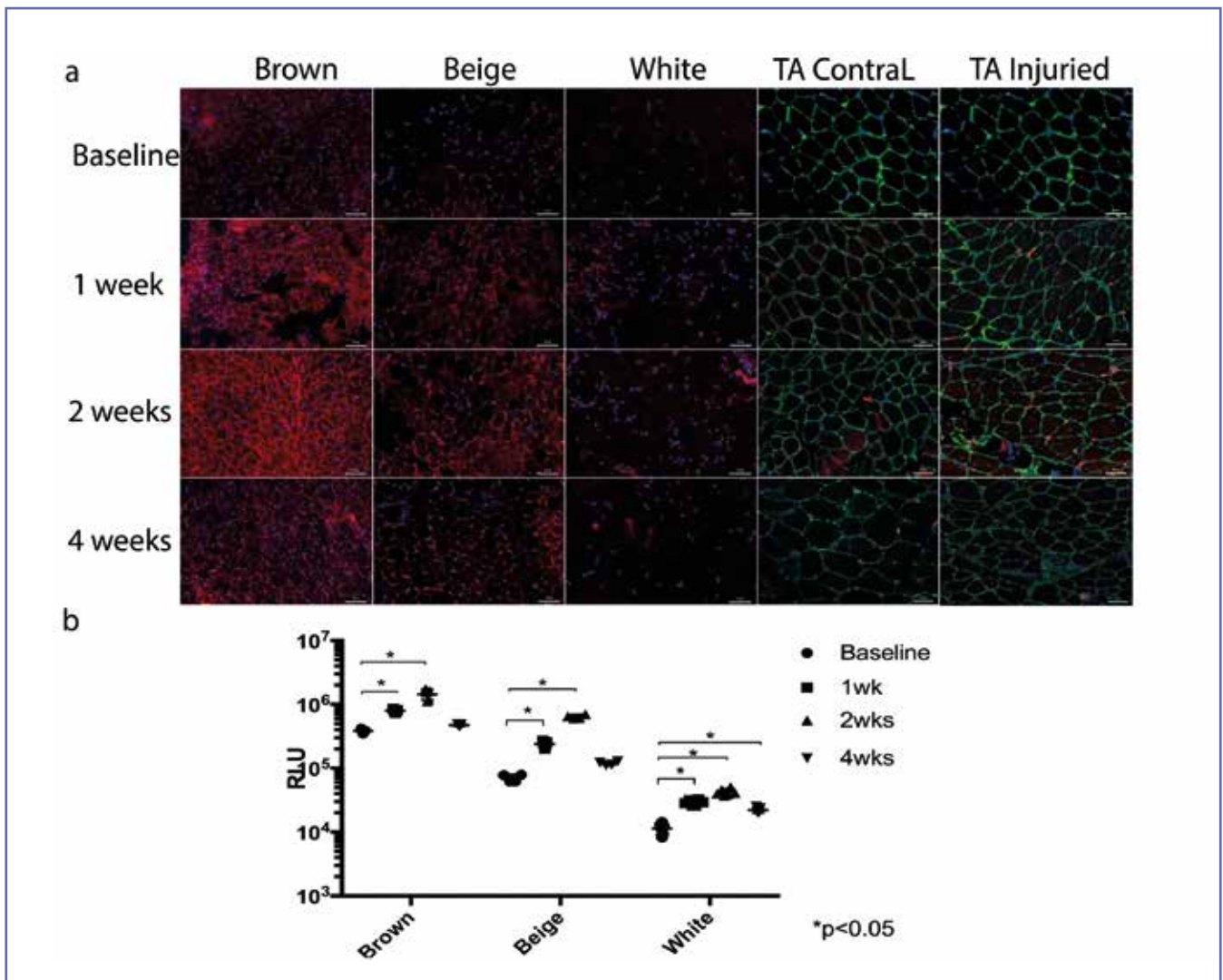
were increased at both 1 week, 2 weeks and 4 weeks after IRI compared to control (**figure 1 a**). The signal intensity peaked at 2 weeks in adipose tissue and decreased at 4 weeks compared to the 2 weeks time point. Moreover, the UCP-1 signal was also detected in both contralateral and injured TA. The UCP-1 signal intensity peaked at 2 weeks and decreased at 4 weeks after IRI (**figure 1 a**). Interestingly, contralateral injured TA muscle had a higher percentage of UCP-1 expressing cells compared to the injured TA muscle (**figure 1 a**). Luciferase assay confirmed findings from histology. UCP-1 driven Luc2 reporter gene expression significantly increased

in brown, beige and white fat, with a peak at 2 weeks after IRI (**figure 1 b**).

RT-PCR showed that, UCP-1 and PRDM-16 expression significantly increased in Brown, Beige and white adipose tissue after IRI (**table II, figure 2**).

**Promyogenic batokine gene expression increased in adipose tissue after IRI**

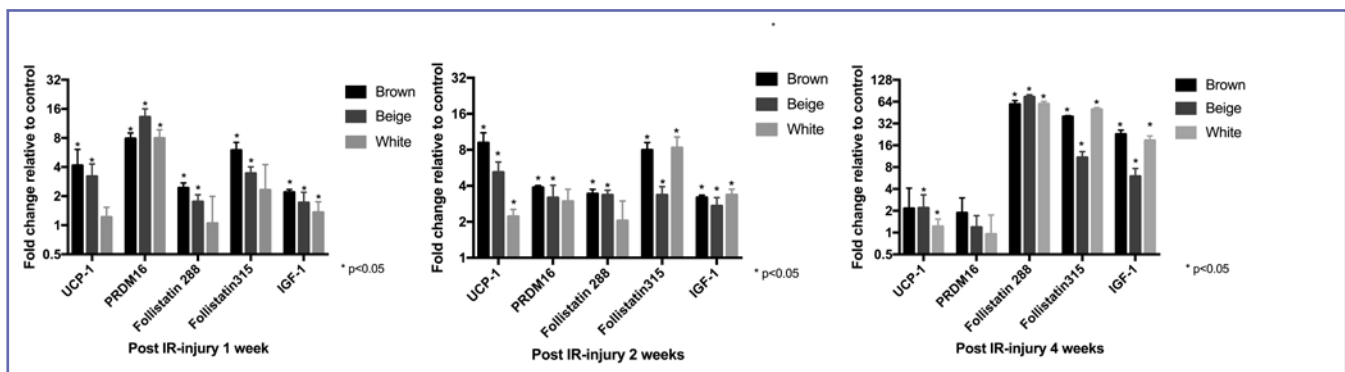
RT-PCR showed that tissue-binding isoform follistatin (Follistatin 288), circulating isoform follistatin (Follistatin



**Figure 1.** (a) Activation of BAT after IRI. Brown, beige, white fat, as well as TA muscle after IRI from UCP-1 reporter mice before (baseline) and at 1, 2, 4 weeks after IRI. Red signal-UCP-1 reporter gene UCP-1 expression increased at 1 and 2 weeks in all types of fat. It decreased to baseline level in brown and beige fat, but remain elevated in white fat at 4 weeks after IRI. (\* p < 0.05).

**Table II.** RT-PCR results of mRNA expression in Brown, Beige and White adipose tissue at 1, 2 and 4 weeks after IR injury. (Mean  $\pm$  SD, \* indicates  $p < 0.05$  compared to baseline control).

1 week	UCP-1	PRDM16	Follistatin 288	Follistatin 315	IGF-1
<b>Brown</b>	4.23 $\pm$ 1.95*	7.87 $\pm$ 1.15*	2.43 $\pm$ 0.31*	5.95 $\pm$ 1.22*	2.19 $\pm$ 0.35*
<b>Beige</b>	3.19 $\pm$ 1.81*	13.18 $\pm$ 2.86*	1.75 $\pm$ 0.19*	3.43 $\pm$ 0.57*	1.71 $\pm$ 0.46*
<b>White</b>	1.11 $\pm$ 0.48	7.95 $\pm$ 1.79*	1.05 $\pm$ 0.94*	2.32 $\pm$ 1.91	1.36 $\pm$ 0.27*
2 weeks	UCP-1	PRDM16	Follistatin 288	Follistatin 315	IGF-1
<b>Brown</b>	9.15 $\pm$ 2.26*	3.87 $\pm$ 0.46*	3.35 $\pm$ 0.37*	7.98 $\pm$ 1.27*	3.19 $\pm$ 0.53*
<b>Beige</b>	5.19 $\pm$ 1.10*	3.18 $\pm$ 0.86*	3.41 $\pm$ 0.17*	3.55 $\pm$ 0.68*	2.71 $\pm$ 0.24*
<b>White</b>	2.21 $\pm$ 0.32*	2.95 $\pm$ 1.97	2.06 $\pm$ 1.44	8.36 $\pm$ 2.03*	3.36 $\pm$ 0.38*
4 weeks	UCP-1	PRDM16	Follistatin 288	Follistatin 315	IGF-1
<b>Brown</b>	2.15 $\pm$ 1.29	1.87 $\pm$ 1.13	59.12 $\pm$ 7.14*	39.48 $\pm$ 1.38*	22.75 $\pm$ 3.13*
<b>Beige</b>	2.32 $\pm$ 0.28*	1.18 $\pm$ 0.56	74.38 $\pm$ 5.31*	10.47 $\pm$ 2.47*	5.96 $\pm$ 1.69*
<b>White</b>	1.16 $\pm$ 0.13	0.95 $\pm$ 0.48	59.68 $\pm$ 4.95*	49.29 $\pm$ 3.14*	18.65 $\pm$ 2.87*

**Figure 2.** UCP-, PRDM-16, IGF1 and follistatin were significantly increased after 1 week, 2 weeks, and 4 weeks IR injury.

315) and IGF1 gene expression level increased in brown, beige and white adipose tissue after IRI (**table II**, **figure 2**).

#### UCP-1 (-/-) mice had reduced muscle regeneration compared to UCP-1 (+/+) WT mice after IRI

DigiGait analysis showed that the swing stride of hind limb increased by 18% ( $p < 0.05$ ), the brake stride decreased

by 28% ( $p < 0.05$ ), the stance stride decreased by 26% ( $p < 0.05$ ) and the stance/swing ratio decreased by 3 folds ( $p < 0.05$ ) in the UCP-1 (-/-) mice compared to UCP-1 (+/+) wildtype mice at two weeks after IRI (**figure 3**).

Muscle histology analysis showed that the regenerating index of TA in UCP-1 (-/-) mice was significantly lower than UCP-1 (+/+) wildtype mice at two weeks after IRI (**figure 4**). The mean of cross section area of myofiber of TA on the injured side in UCP-1 (-/-) mice at two weeks

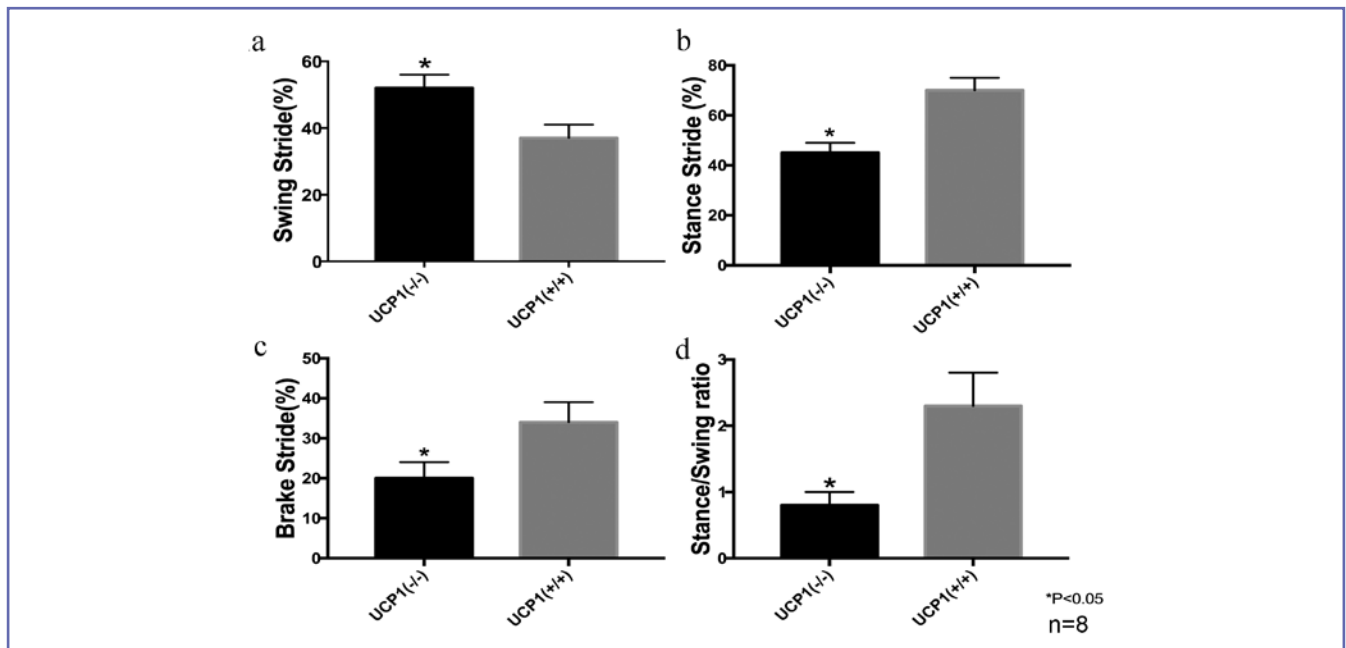


**Figure 3.** UCP-1 (-/-) mice have significantly increased swing stride and reduced stance stride, brake stride and stance/swing ratio compared to Wildtype (WT) mice at 2 weeks after IRI.

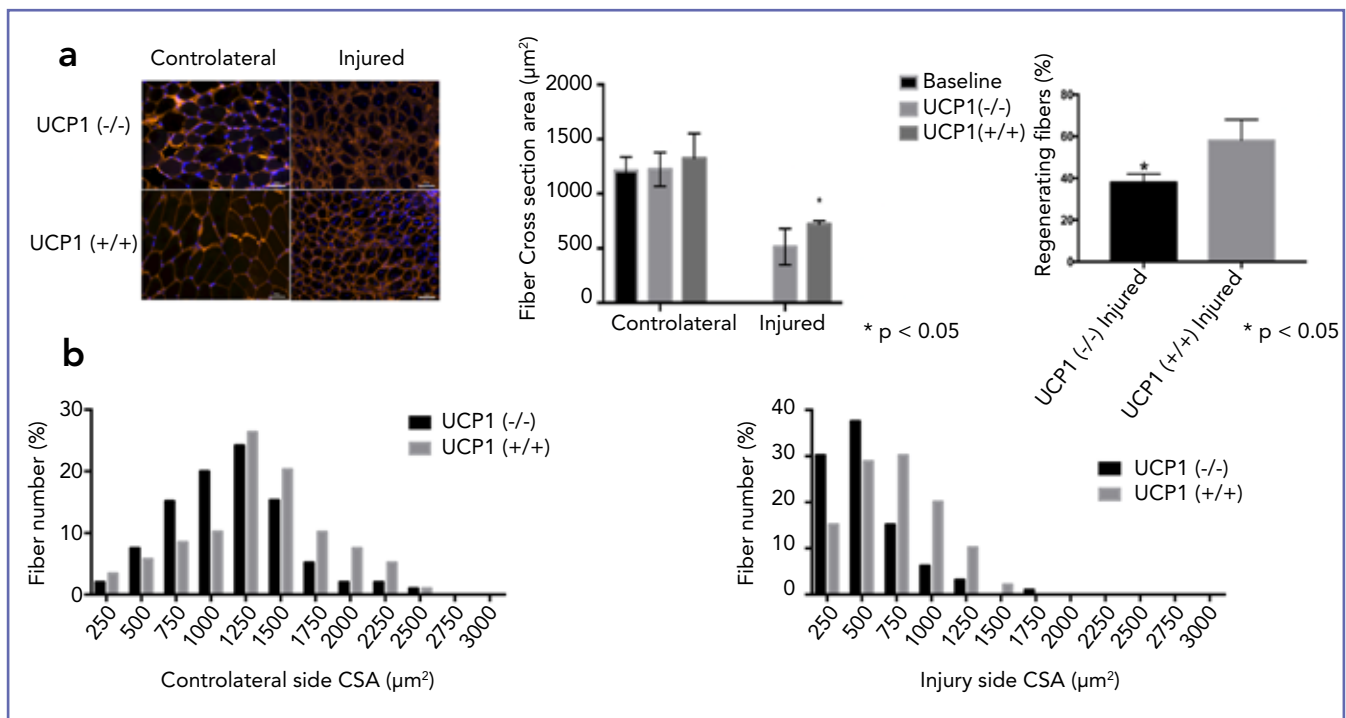


**Figure 4.** (a) UCP-1 (-/-) mice have significantly reduced regenerating fibers ratio (% of central nuclei regenerating fiber number/ total fiber number) and average muscle fiber cross section area at 2 weeks after IRI compared to UCP-1 (+/+) wildtype mice. (Scale bar stands for 50 μm). (\* p < 0.05 compared to WT mice). (b) Histogram of muscle fiber cross-section area of TA muscles at contralateral and IRI sides of UCP-1 (-/-) and UCP-1 (+/+) mice at 2 weeks after IRI.

(513.15  $\mu\text{m}^2$ ) was significantly smaller than that in UCP-1 (+/+) mice (720.625  $\mu\text{m}^2$ ), though no significant difference was found at the contralateral uninjured TA (1324.5  $\mu\text{m}^2$  in UCP-1 (+/+) mice *vs.* 1222.75  $\mu\text{m}^2$  in UCP1 (-/-) mice (figure 4).

### Amibegron improved hindlimb muscle regeneration after IRI

DigiGait analysis showed that, compared to DMSO vehicle-treated mice, mice treated with Amibegron had significantly increased stance width ( $p=0.03$ ) and stride length ( $p=0.03$ ) at 4 weeks after IRI (figure 5).

Muscle histology showed that the average regeneration index in TA of Amibegron treated mice was significantly higher than that in DMSO treated mice ( $p=0.04$ ) (figure 6 a). Four weeks treatment of Amibegron also significantly increased mean cross section area of myofiber of TA after IRI (1113.15  $\mu\text{m}^2$  in Amibegron group compared to 892.20  $\mu\text{m}^2$  in DMSO group,  $p=0.01$ ) (figure 6 a, c). Finally, the brown fat markers were increased in Amibegron treated group compared to DMSO in brown, beige, white adipose tissue. The batokines were increased significantly as well (figure 6 b).

## DISCUSSION

Skeletal muscle and adipose tissue are made up large portion of human body. An average adult male has 42% as the skeletal muscle and an average adult female has 36% (a percentage of body mass) (12). The mean percentage of body fat ranges from 22.9% to 30.9% in adult males and from 32.0% to 42.4% in adult females. Despite increasing knowledge of cross-talk between muscle and fat, our understanding of interactions between these two biggest organs in our body remains limited. In this study, we have observed significant morphology and gene expression change in adipose tissue, including brown/beige fat activation and white fat “browning” after muscle Ischemia-Reperfusion Injury (IRI). Mice with non-functional BAT by knocking out UCP-1 have significantly reduced muscle regeneration. These new finding suggests a novel interaction between fat and muscle, that BAT promotes muscle regeneration after IRI.

Brown/Beige Adipose Tissue (BAT) is the main site of adaptive thermogenesis (13). Reduction of blood flow after IRI can lead to reduced temperature in the injured limb. Thus, activation of BAT after IRI may be a natural reaction to muscle IRI in response to increased need of thermogenesis, especially at early stage after injury. However, BAT possesses more functions other than thermogenesis. Recent studies

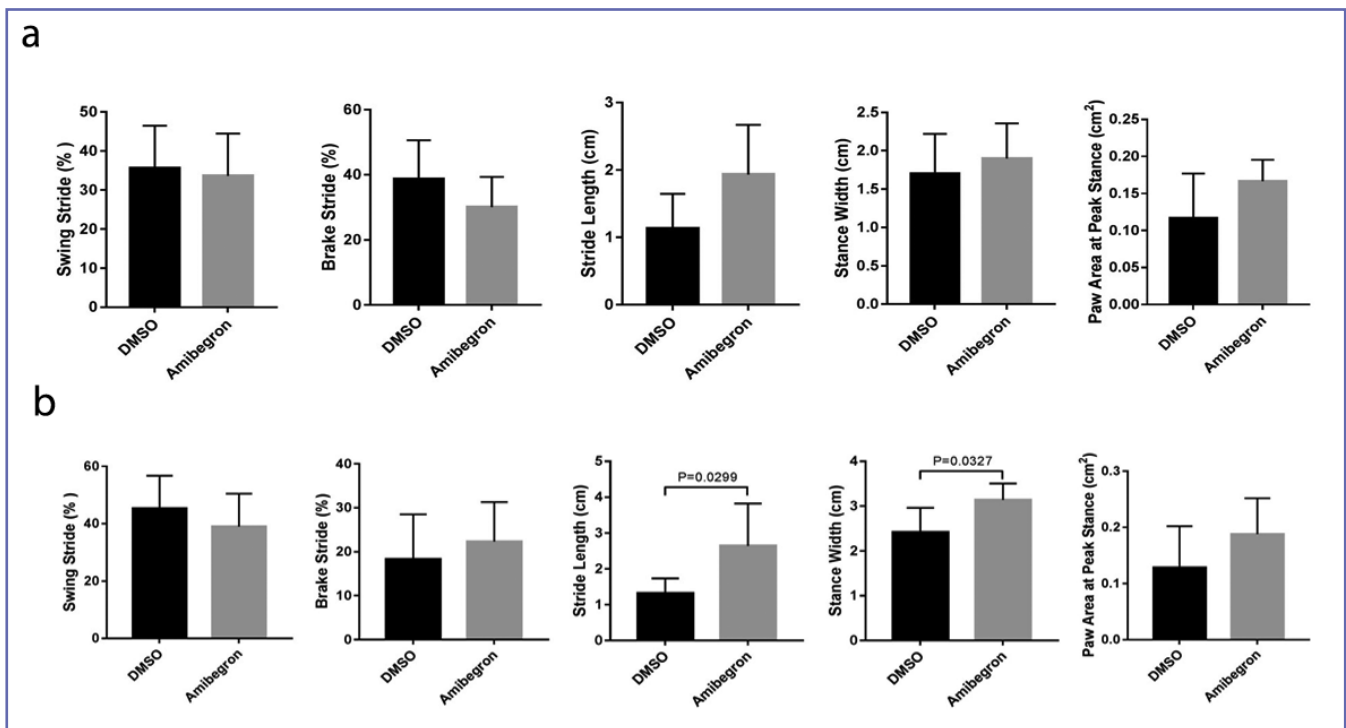


**Figure 5.** DigiGait analysis at 2 weeks (a) and 4 weeks (b) after IRI showed that Amibegron improves injured hindlimb limb function at 4 weeks after IRI.

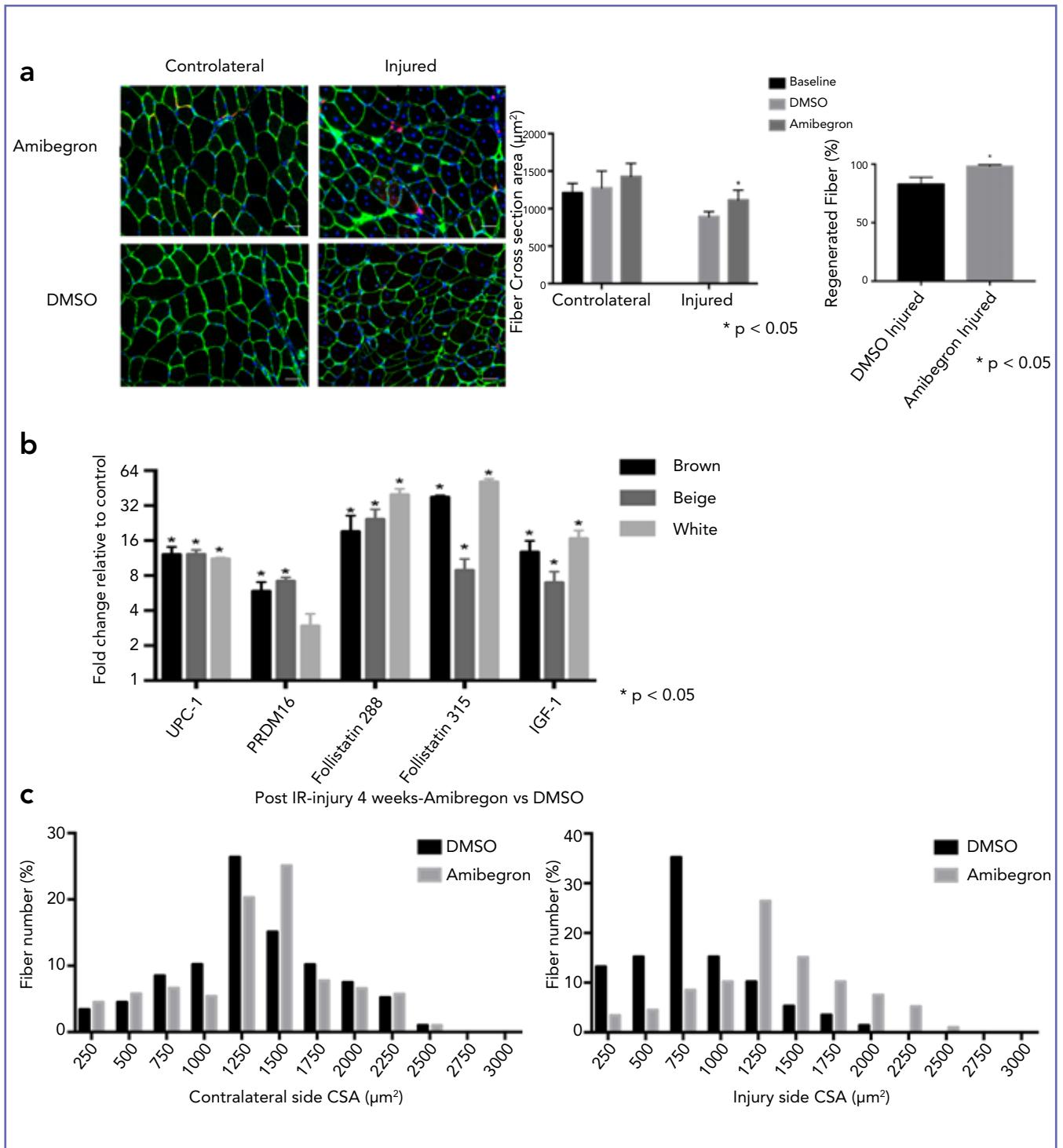


**Figure 6.** (a) Mice receiving Amibegron treatment for 4 weeks have significantly higher regenerating fiber % and average muscle fiber cross-section area after IRI compared those received DMSO (vehicle for Amibegron) (scale bar stands for 50  $\mu\text{m}$ ). (b) UCP1, PRDM-16, follistatin and IGF-1 expression significant increased compared to DMSO group. (c) Histogram of muscle fiber cross-section area of TA muscles at contralateral and IRI sides on mice with Amibegron and DMSO treatment at 4 weeks after IRI.



have been shown that BAT also has a secretory role, which could contribute to the systemic consequences of BAT activity. An increasing body of BAT-derived cytokines (namely batokine) have been identified as paracrine or endocrine factors (5, 14). In this study, we found significantly increased expression of IGF1 and follistatin, two important promyogenic batokines from BAT after muscle IRI, suggesting BAT may facilitate muscle regeneration after IRI through paracrine/endocrine function of promyogenic batokines.

It is interesting that we found thermogenesis regulated genes, including UCP-1 and PRDM-16 increased in BAT at relative early stage (1-2 weeks) after muscle IRI while promyogenic batokine (including follistatin and IGF1) gene expression were highly up-regulated at later stage (4 weeks) after IRI. This data suggests that BAT may facilitate mice recovery after IRI at two phases: thermogenesis in early stage and paracrine/endocrine of promyogenic batokines in late stage after IRI.

Epididymal fat pad in adult mice is considered a typical source of white fat. However, in this study, we saw remarkable UCP-1 reporter signal in epididymal fat pad after IRI. Though significantly lower than that in brown and beige fat, UCP-1 signal in epididymal fat remained increased even at 4 weeks after IRI. Expression of BAT markers, including UCP-1 in white fat is known as “white fat browning”. Browning of white fat is accompanied with metabolism changes and energy consumption. Thus, white fat browning has been considered as new hope to treat obesity and type II diabetics. White fat browning is induced with drugs, exercise and cold inducement (15). In this study, we observed spontaneous white fat brown after muscle IRI. This suggests a dramatic change in metabolism after muscle IRI. Expression of promyogenic factors of follistatin and IGF1 also increased in the “browning” white fat, suggesting a possible endocrine role of browning white fat after muscle IRI (16). Besides adipose tissue, we also found UCP-1 signaling in muscle after IRI. Interestingly, UCP-1 (+) BAT cells are not only found in injured muscle, but also within non-injured muscle at the contralateral side. The origin and function of intramuscular BAT after muscle IRI remains unknown at this time. Among all muscle progenitor cells, Fibro-Adipogenic Progenitors (FAPs) are most likely to be the cellular origin of the intramuscular BAT after muscle IRI, due to their adipogenic potential. A recent study showed that FAPs can express UCP-1 *in vitro* and *in vivo* (15, 17). Future work is needed to define the cellular source and function of intramuscular BAT after muscle IRI.

Follistatin (Fst) is a secreted glycoprotein that has a high affinity binding and neutralizing other proteins such as several members of the TGF- $\beta$  superfamily including Activins and Myostatin (Mst). Follistatin has reported isoforms

FST288, FST315, and FST300 (or FST303). FST288 and FST315 are known to be created by alternative splicing of the FST gene transcript, while FST300 is thought to be the product of posttranslational modification of C-terminal domain truncation. FST315 is primarily found in circulation, whereas FST288 displays greater cell surface affinity. Thus, FST288 is considered to function through an auto-crine fashion while FST315 is more like to play an endocrine role.

Follistatin proteins were found to antagonize Myostatin mediated inhibition of myogenesis (18, 19). FST-transgenic mice produced a robust skeletal muscle hypertrophy phenotype, which proved its promyogenic role *in vivo* (20). Recent work suggests that Fst also promotes BAT differentiation and energy metabolism. Thus, Fst may play a dual role in both promoting muscle growth and inducing BAT activation after muscle IRI. In this study, we have observed significantly increased gene expression of both Fst288 (tissue binding isoform) and Fst315 (circulating isoform) from brown, beige and white fat. Considering their distinguished difference, Fst315 may be responsible for promoting muscle regeneration, while Fst288 may be responsible for BAT activation and white fat “browning”. Future work is needed to define the exact function of Fst288 and Fst315 after muscle IRI.

BAT activity is highly regulated by sympathetic nerves system, mainly through  $\beta_3$  adrenergic receptor pathway.  $\beta_3$  adrenergic receptors are selectively expressed in adipose tissue and  $\beta_3$  adrenergic receptor agonists can effectively stimulate BAT activity in both animals and human (16). In this study, we found that Amibegron, a selective  $\beta_3$  adrenergic receptor agonist significantly improved muscle regeneration and limb function after IRI. This data suggests that selective  $\beta_3$  adrenergic receptor agonists may serve as a new treatment for muscle IRI. Mirabegron, a selective  $\beta_3$  adrenergic receptor agonist with a similar structure to Amibegron, has been approved by the FDA for treating over-reactive bladders (21). Mirabegron could be considered as a potential novel treatment to improve muscle regeneration after IRI.

Some limitations of this study should be noted. First of all, the effect of species differences on quantity of BAT between mouse and human is significant. Adult mice contain a significant amount of BAT, while the amount of BAT in adult humans is relatively small. Most BAT tissues in adult human remain inactive without appropriate physical or chemical stimulations. Second, we only used RT-PCR to investigate promyogenic batokine expression in adipose tissue in this study. To quantify the protein of batokines in both adipose tissue and circulation is needed in future works. Third, due to limited supply of knockout mice, we only employed

UCP-1 knockout mice at one time point (2 weeks) after IRI. Though the results are convincing, we will consider employing other time points when more knockout mice become available in the future. Last but not least, because the UCP-1<sup>luc2-dtTomato</sup> reporter gene was inserted on to the Y chromosome in UCP-1 reporter mice, we predominantly used male mice in this study. Finding in this study needs to be verified on female mice in the future.

## CONCLUSIONS

Results from this study suggest that BAT plays an important role in muscle regeneration of IRI. Pro-myogenic batokines from BAT may be the mediator for muscle regeneration after IRI.  $\beta_3$  adrenergic receptor agonists may be novel treatment for muscle IRI in the future.

## ACKNOWLEDGEMENTS

This work was supported by VA BLR&D Merit review grant (1 I01 BX002680-01A2) (PI: Kim) and a pilot research grant from UCSF Core Center for Musculoskeletal Biology and Medicine (NIH 1P30AR066262-01) (PI: Brian Feeley). Zili Wang was supported by the China Scholarship Council to study at the University of California, San Francisco.

## CONFLICT OF INTERESTS

The authors declare that they have no conflict of interests.

## REFERENCES

- Gillani S, Cao J, Suzuki T, Hak DJ. The effect of ischemia reperfusion injury on skeletal muscle. *Injury* 2012;43(6):670-5.
- Kalogeris T, Baines CP, Krenz M, Korthuis RJ. Cell biology of ischemia/reperfusion injury. *Int Rev Cell Mol Biol* 2012;298:229-317.
- Giralt M, Villarroya F. White, brown, beige/brite: different adipose cells for different functions? *Endocrinology* 2013;154(9):2992-3000.
- Villarroya J, Cereijo R, Villarroya F. An endocrine role for brown adipose tissue? *Am J Physiol Endocrinol Metab* 2013;305(5):E567-72.
- Trayhurn P, Drevon CA, Eckel J. Secreted proteins from adipose tissue and skeletal muscle - adipokines, myokines and adipose/muscle cross-talk. *Arch Physiol Biochem* 2011;117(2):47-56.
- Shaw JC, Wilson FC. Radial perilunar dislocation. Report of a case. *J Bone Joint Surg Am* 1970;52(3):556-8.
- Kaur KK. Advances in BAT physiology for understanding and translating into Pharmacotherapies for obesity and comorbidities. *MOJ Drug Des Devel Ther* 2018;2(5):10.
- Joshi SK, Lee L, Lovett DH, *et al.* Novel intracellular N-terminal truncated matrix metalloproteinase-2 isoform in skeletal muscle ischemia-reperfusion injury. *J Orthop Res* 2016;34(3):502-9.
- Padulo J, Oliva F, Frizziero A, Maffulli N. Muscle, Ligaments and Tendons Journal - Basic principles and recommendations in clinical and field. *Science Research: 2018 update. MLTJ* 2018;8(3):305-307.
- Wang Z, Liu X, Davies MR, Horne D, Kim H, Feeley BT. A Mouse Model of Delayed Rotator Cuff Repair Results in Persistent Muscle Atrophy and Fatty Infiltration. *Am J Sports Med* 2018;46(12):2981-9.
- Manthorpe M, Cornefert-Jensen F, Hartikka J, *et al.* Gene therapy by intramuscular injection of plasmid DNA: studies on firefly luciferase gene expression in mice. *Hum Gene Ther* 1993;4(4):419-31.
- Marieb NE, Hoehn K. *Human Anatomy & Physiology*, 8 ed. San Francisco: Benjamin Cummings, 2010:pp. 312.
- Fenzl A, Kiefer FW. Brown adipose tissue and thermogenesis. *Horm Mol Biol Clin Investig* 2014;19(1):25-37.
- Villarroya F, Cereijo R, Villarroya J, Giralt M. Brown adipose tissue as a secretory organ. *Nat Rev Endocrinol* 2017;13(1):26-35.
- Aldiss P, Betts J, Sale C, Pope M, Budge H, Symonds ME. Exercise-induced 'browning' of adipose tissues. *Metabolism* 2018;81:63-70.
- Cypess AM, Weiner LS, Roberts-Toler C, *et al.* Activation of human brown adipose tissue by a  $\beta_3$ -adrenergic receptor agonist. *Cell Metab* 2015;21(1):33-8.
- Gorski T, Mathes S, Krutzfeldt J. Uncoupling protein 1 expression in adipocytes derived from skeletal muscle fibro/adipogenic progenitors is under genetic and hormonal control. *J Cachexia Sarcopenia Muscle* 2018;9(2):384-99.
- Hill JJ, Davies MV, Pearson AA, *et al.* The myostatin propeptide and the follistatin-related gene are inhibitory binding proteins of myostatin in normal serum. *J Biol Chem* 2002;277(43):40735-41.
- Thomas M, Langley B, Berry C, *et al.* Myostatin, a negative regulator of muscle growth, functions by inhibiting myoblast proliferation. *J Biol Chem* 2000;275(51):40235-43.
- Lee SJ, Huynh TV, Lee YS, *et al.* Role of satellite cells versus myofibers in muscle hypertrophy induced by inhibition of the myostatin/activin signaling pathway. *Proc Natl Acad Sci U S A* 2012;109(35):E2353-60.
- Rossanese M, Novara G, Challacombe B, Iannetti A, Dasgupta P, Ficarra V. Critical analysis of phase II and III randomised control trials (RCTs) evaluating efficacy and tolerability of a beta(3)-adrenoceptor agonist (Mirabegron) for overactive bladder (OAB). *BJU Int* 2015;115(1):32-40.